IC/85/179
INTERNAL REPORT
(Limited distribution)

International Atomic Energy Agency
and
United Nations Educational Scientific and Cultural Organization

INTERNATIONAL CENTRE FOR THEORETICAL PHYSICS

AN ANALYSIS OF HEAT FIELD OF METAL SHEET DURING ELASTIC-PLASTIC DEFORMATION *

S.X. Li
College of Heavy Machines, Taiyuan, People's Republic of China

Y. Huang
International Centre for Theoretical Physics, Trieste, Italy
and
Institute of Metal Research, Academia Sinica, Shenyang,
People's Republic of China **

and

C.H. Shih
Institute of Metal Research, Academia Sinica, Shenyang,
People's Republic of China.

MIRAMARE - TRIESTE
August 1985

* Submitted for publication.

** Permanent address.

ABSTRACT

This paper describes the application of the finite element analysis to calculate the temperature distribution generated during the process of elastic-plastic deformation.

A better agreement is found between the results of heat field computed by use of the finite element analysis and that measured by use of infrared camera. The results indicate that the method of finite element analysis used for heat field evaluation is reliable.

I. INTRODUCTION

In recent years linear elastic fracture mechanics acquired very important achievements on the theoretical research as well as on the practical and industrial applications. However, in the construction materials or engineering materials with higher plasticity and toughness, the damage and fracture usually take place on the condition of elastic-plastic or even totally plastic. In this case, even the revised linear elastic fracture mechanics is not applicable.

For example, the J integral and COD (Crack Opening Displacement) have achieved significant advances on the criterion of elastic-plastic fracture. But, until quite recently there are many controversies both on the theory and experimental techniques. Therefore, investigation of elastic-plastic deformation process at different angles is commendatory.

There is a general concern regarding the heat phenomenon of the constructional materials during deformation. Some results of heat phenomenon at the crack tip in the elastic zone have been obtained in the adiabatic condition by Williams[1]. Weichert and Schoenert [2] have investigated heat generated by fast propagation of cracks in non-metallic materials. However, they were unable to consider the influence of thermal-conduction which is important during quasi-static deformation process. The previous works have principally conducted model-tests and measurements of heat field of metal during deformation. Theoretical calculations have only been based on simplified assumptions [3]. During recent years, the theoretical research and measurement of the heat field of metal during deformation could be improved due to the development of the computer science and application of the finite element method, and application of technique of real-time measurement temperature field.

In this paper, finite element analysis was used to calculate temperature distribution generated during elastic-plastic deformation of the metal sheet. The practical patterns of heat field of the metal sheet during elastic-plastic deformation were given by use of the infrared thermographic. A good agreement has been obtained between the results of calculation and those of experiments.

II. THE PRINCIPLE

In general, the temperature change T with variety of strain tensor ε in the range of elastic deformation can be expressed by Kelvin's formula [3]

$$\frac{\partial}{\partial x_i}\left(k_{ij}\frac{\partial T}{\partial x_j}\right)=\rho c_v\frac{\partial T}{\partial t}+T\beta_{ij}\frac{\partial \varepsilon_{ij}}{\partial t}$$
$$(i,\ j=1,\ 2,\ 3) \qquad , \qquad (1)$$

where x_i is the geometry coordinates of subject; k_{ij} the thermal conductivity tensor; ε_{ij} the strain tensor; β_{ij} the tensor of material property; ρ the density; c_v the specific heat at constant pressure and t the time. For the homogeneous and isotropic materials, in Eq.(1) the thermal conductivity tensor $k_{ij}=k\delta_{ij}$; $\beta_{ij}=\beta\delta_{ij}$, here $\beta=\frac{\alpha E}{1-2\nu}$, where δ_{ij} is the Kronecker operator, α the linear expansion coefficient, E the modules of elasticity and ν the Poisson ratio. In the adiabatic situation, Eq.(1) becomes

$$\frac{\partial T}{\partial t}=-\frac{T}{\rho c_v}\beta_{ij}\frac{\partial \varepsilon_{ij}}{\partial t} \qquad . \qquad (2)$$

The Kelvin formula has been confirmed experimentally [4]. The drop in temperature of the metal sheet during elastic deformation confirmed that Eq.(2) was correct, too [5], as shown in Fig.1.

It is assumed that the Fourier thermal conductance law is still valid in the range of elastic-plastic deformation, then an unsteady heat conductance control equation can be set up as

$$\rho c_v\frac{\partial T}{\partial t}=\frac{\partial}{\partial x_i}\left(k_{ij}\frac{\partial T}{\partial x_j}\right)+\dot{Q} \qquad , \qquad (3)$$

where $\dot{Q}$ is the rate of heat generation per unit volume. However, the anisotropy of material is more pronounced after plastic deformation, so the heat conductivity and consequently the heat distribution will vary with strain as shown in Fig.2.

The experiments show that the change of the thermal conductivity is less than 16% with value of strain ε from zero rises to 0.15. The calculation is only limited to low deformation, the strain being less than 0,05. So that the thermal conductivity can be considered unvariable and the error is not larger than 5%, thus Eq.(3) can be reduced as

$$\rho c_v\frac{\partial T}{\partial t}=k\nabla^2 T+\dot{Q} \qquad , \qquad (4)$$

where, $\dot{Q}=\dot{Q}_e+\dot{Q}_p$; $\dot{Q}_e$ the rate of heat generation per unit volume due to elastic deformation, $\dot{Q}_p$ the rate of heat generation per unit volume due to plastic deformation. From Eq.(1), $\dot{Q}_e=-T\beta_{ij}\frac{\partial \varepsilon_{ij}}{\partial t}$. Here we considered that the part of elastic deformation is still producing the heat effect. Even

if $\dot{Q}_p$, it is well known that a large amount of plastic work is converted into heat due to the dislocation moving, crystal slipping during plastic deformation. The rate of plastic heat generation per unit volume is then given by [6]

$$\dot{Q}_p=\mu\bar{\sigma}\dot{\bar{\varepsilon}}_p \qquad , \qquad (5)$$

where $\bar{\sigma}$ is the equivalent stress; $\dot{\bar{\varepsilon}}_p$ the equivalent rate of plastic strain; μ the coefficient of conversion from plastic deformation to heat (here $\mu=0.95$). The problem is now how to calculate $\dot{Q}_p$, and the finite element analysis method has been tried.

III. THE CALCULATION OF ELASTIC PLASTIC DEFORMATION FIELD AND HEAT FIELD

3.1 Calculation of Deformation Field

Based on the Von Mises yield criterion, the Prandl-Reuss equation of the increment theory has been adopted, so the differential equations is given by

$$de_{ij}=\frac{1}{2G}ds_{ij}+d_\lambda s_{ij} \qquad , \qquad (6)$$

where $e_{ij}=\varepsilon_{ij}-\varepsilon_m\delta_{ij}$ the strain partial amount ($\varepsilon_m=\varepsilon_{ij}/3$ the mean strain); $s_{ij}=\sigma_{ij}-\sigma_m\delta_{ij}$ the stress partial amount ($\sigma_m=\sigma_{ij}/3$ the mean stress); d_λ the unnegative coefficient; G the modules of shearing. In order to calculate finite element analysis conveniently, d_λ has disappeared from Eq.(6) and the above equation can be converted into [7]

$$d\{\varepsilon\}_p=\frac{\partial\bar{\sigma}}{\partial\{\sigma\}}d\bar{\varepsilon}^p \qquad , \qquad (7)$$

where $\{\varepsilon\}=\{\varepsilon_x^p,\varepsilon_y^p,\varepsilon_z^p,\gamma_{xy}^p,\gamma_{yz}^p,\gamma_{zx}^p\}^T$

$$\frac{\partial\bar{\sigma}}{\partial\{\sigma\}}=\left\{\frac{\partial\bar{\sigma}}{\partial\sigma_x},\ \frac{\partial\bar{\sigma}}{\partial\sigma_y},\ \frac{\partial\bar{\sigma}}{\partial\sigma_z},\ \frac{\partial\bar{\sigma}}{\partial\tau_{xy}},\ \frac{\partial\bar{\sigma}}{\partial\tau_{yz}},\ \frac{\partial\bar{\sigma}}{\partial\tau_{zx}}\right\}^T$$

$$d\bar{\varepsilon}^p=\sqrt{\frac{2}{3}}\left\{d\varepsilon_x^{p^2}+d\varepsilon_y^{p^2}+d\varepsilon_z^{p^2}+\frac{1}{2}\left(d\gamma_{xy}^{p^2}+d\gamma_{yz}^{p^2}+d\gamma_{zx}^{p^2}\right)\right\}^{1/2}$$

T the transpose of a matrix; $d\varepsilon_{ij}^p$ the plastic strain increment.

When we considered the deformation hardness of material, it is necessary to lead the hardness condition

$$\bar{\sigma} = H(\int d\bar{\varepsilon}^{p}) \quad . \tag{8}$$

Then we can obtain the equation as follows:

$$d\{\sigma\} = [D]_{ep} d\{\varepsilon\} \quad , \tag{9}$$

where $[D]_{ep}$ is the elastic-plastic matrix, that is, $[D]_{ep} = [D]_{e} - [D]_{p}$, $[D]_{e}$ the elastic matrix and plastic matrix

$$[D]_{p} = \frac{[D]_{e} \frac{\partial \bar{\sigma}}{\partial \{\sigma\}} \cdot \left\{\frac{\partial \bar{\sigma}}{\partial \{\sigma\}}\right\}^{T} \cdot [D]_{e}}{H' + \left\{\frac{\partial \bar{\sigma}}{\partial \{\sigma\}}\right\}^{T} \cdot [D]_{e} \cdot \frac{\partial \bar{\sigma}}{\partial \{\sigma\}}} \quad .$$

Here H' is able to obtain from the stress-strain curve during tensile testing [8].

During the process of every step loading, according to the elastic zone, the plastic zone and the transition zone, the element hardness matrix $[k_{el}]$ can be calculated. The total stiffness matrix $[K]$ is the sum of element stiffness matrix $[k_{el}]$

$$[K] = \sum_{1}^{el} [k_{el}] \quad . \tag{10}$$

We adopted the variable stiffness method. When the initial load starts, the initial stress and strain were unexistence, the relation of elastic stress-strain can be written by use of increment form

$$\Delta\{\sigma\} = [D]_{e} \Delta\{\varepsilon\} \quad . \tag{11}$$

In terms of the finite element form, the balance equation can be given as

$$[K]\Delta\{\delta\} = \Delta\{F\} \quad , \tag{12}$$

where $\Delta\{\delta\}$ the node displacement increment and $\Delta\{F\}$ the increasing node load vector.

Therefore, if the displacement increment of every node $\Delta\{\delta\}$ is solved, then the strain increment of every element $\Delta\{\varepsilon\}$ can be given from the equation $\Delta\{\varepsilon\} = [B]^{el}\Delta\{\delta\}$ (here $[B]^{el}$ is the element geometry matrix), and the stress increment of element $\Delta\{\sigma\}$ can be obtained by use of Eq.(11). After element yielding, the total stiffness matrix $[K]$ has a variation. So Eq.(11) is not applicable, but Eq.(9) can still be adopted. It has to be noted that the $[D]_{ep}$ of Eq.(9) is related to the stress levels calculated. So that Eq.(9) is unlinear, but it can be solved by use of increased loading step by step. During the process of plastic deformation Eq.(12) can also be used. In order to calculate the value of load p which takes part in the initial plastic deformation of any element, to order of the elastic-limit load p_e, the loading p-Δp has been divided into n sections, and then the calculation is carried out section by section until all of the loading can be finished. So the stress increment at each section $\Delta\{\sigma\}$, strain increment $\Delta\{\varepsilon\}$, displacement increment $\Delta\{\delta\}$ can be obtained and hence also the values of stress, strain and displacement.

On the experimental load-time curve there is a time increment Δt which agrees with the loading increment Δp, therefore the rate of plastic heat generation per unit volume $\dot{Q}_p$ at each section can be obtained and then $\dot{Q}$ can also be calculated.

3.2 Calculation of Heat Field

In this paper, we only considered the plate problem. If there is a plate body of unit thickness and the thermal conduction takes place in the plate zone R (see Fig.3). The rate of temperature rise at some time in subzone F is $\partial T/\partial t$, the consumed heat for temperature rise at dt time is given by

$$dQ_1 = \int_F \frac{\partial T}{\partial t} dt C_v \rho dA \quad . \tag{13}$$

The heat supplied by heat sound of the same subzone is as follows:

$$dQ_2 = \int_F -T\beta_{uv}\frac{\partial \varepsilon_{uv}}{\partial t}\,dA\,dt + \int_F \mu\bar{\sigma}\dot{\bar{\varepsilon}}\,dA\,dt \quad , \qquad (14)$$

where $u,v = 1,2,3$; A the area of unit element. The heat transferred into the same subzone which passes through the round line l can be written as

$$dQ_3 = \oint_l k\frac{\partial T}{\partial n}\,ds\,dt \quad . \qquad (15)$$

If F is a boundary subzone in plate zone R, then the released heat which passes boundary round line c at dt time is

$$dQ_4 = \int_c \beta_0(T - T_a)\,ds\,dt \quad , \qquad (16)$$

where β_0 the coefficinet of released heat and T_a the around medium temperature. For the metal thin sheet, the released heat of two sides of the specimen can be expressed as

$$dQ_5 = 2\int_F \beta_0(T - T_a)\,dA\,dt \quad . \qquad (17)$$

Here we utilized the triangular subdivided and the linear temperature model as in the calculation of elastic-plastic deformation. The zone surrounded by midside node i and with centre at every element is regarded as the zone of node i. The node temperature is served as common temperature of the zone. In this case, based on Eqs.(13) and (17) and integrating with heat balance principle, we obtain the hidden difference equation for internal node i

$$\Big(\sum_e c_v\rho A\Big)T_{i,t} + \frac{3\Delta t}{4}\sum_e \frac{k}{A}[(b_i^2 + c_i^2)T_{i,t} + (b_i b_j + c_i c_j)T_{j,t}$$
$$+ (b_i b_m + c_i c_m)T_{m,t}] + 2\Delta t\Big(\sum_e \beta_0 A\Big)T_{i,t} = \Big(\sum_e c_v\rho A\Big)T_{i,t-\Delta t}$$
$$+ \sum_e \mu\bar{\sigma}\dot{\bar{\varepsilon}}_p A + \sum_e (-T_i\beta_{uv}\Delta\varepsilon_{uv})A + 2\Delta t\sum_e \beta_0 A T_a \quad . \qquad (18)$$

The hidden difference equation for bound node i

$$\Big(\sum_e c_v\rho A\Big)T_{i,t} + \frac{3\Delta t}{4}\sum_e \frac{K}{A}\Big[(b_i^2 + c_i^2)T_{i,t} + (b_i b_j + c_i c_j)T_{j,t} +$$
$$+ (b_i b_m + c_i c_m)T_{m,t}\Big] + 2\Delta t\Big(\sum_e \beta_0 A\Big)T_{i,t} + \frac{3}{2}\beta_0(L_1 + L_2)\Delta t\,T_{i,t} =$$
$$= \Big(\sum_e c_v\rho A\Big)T_{i,t-\Delta t} + \sum_e \mu\bar{\sigma}\Delta\dot{\bar{\varepsilon}}_p A + \sum_e (-T_i\beta_{uv}\Delta\varepsilon_{uv})A + 2\Delta t\sum_e \beta_0 A T_a +$$
$$+ \frac{3\Delta t}{2}\beta_0(L_1 + L_2)T_a \quad , \qquad (19)$$

where $\sum_e$ represent the sum of all elements which surrounded node i; b_i, c_i, b_j, c_j, b_m, c_m the element geometry character length; T_j, T_m the node temperature of two remaining nodes of element and l_1, l_2 the boundary length of bound element.

These equations are linear algebra ones. The node temperature after a moment t can be solved from that at time $t-\Delta t$ and the variation of heat field can also be decided, due to the hidden difference equations have stable solution [9].

The preparative stages of the calculation are as follows: (i) the tensile stress-strain curves of material are measured from experimental test; (ii) the tensile load-time curve of material is set up to experiment or to assumed calculation model and (iii) to make the source programmes of computer.

IV. THE CALCULATED RESULTS

In order to study the heat distribution generated during the elastic-plastic deformation of the metal sheet, the specimens have centre circle hole, rhomb hole (120°) and twins saw cut-hole (ϕ 0.2 mm), respectively. The geometry forms of specimen are given in Fig.4. In this case, the specimens stand in plate stress condition due to the thickness being less than the width of specimen. Because of symmetric condition of mechanic and thermodynamics of specimen, the quarter of one was regarded as the calculated model (the size of calculated area is 15 mm^2). We adopt the triangular element subdivided, linear displacement model and linear temperature model, and the typical subdivisions of three various hole shapes are as 110, 107 and 113 elements, respectively.

The true stress-strain curve of the stainless steel and the tensile load-time curve were measured from testing, while the tensile rate was 25mm/min as shown in Figs.5 and 6. When the plastic zone extended to the boundary, the temperature distributions calculated by use of computer are shown in Fig.7. The tensile time of these results just agree with A, B and C point of elastic-plastic deformation in Fig.6. The photographs of infrared image and isotherms of thermographic are shown in Figs.8 and 9, respectively [5].

It may be seen that the calculated results agree with the results of experiment. At this time, the plastic zone is equivalent to the zone in Fig.10 and the equivalent strain at the same time is given in Fig.11.

The isothermal ranges and temperature values of three various hole shapes are different. It turns out that the value of temperature with circle hole is the highest, one of rhomb is second and twins saw-cut the third. Because of the largest plastic work can be transferred into heat during tensile testing, when the plastic zone of the specimen extend to the V position, the circle hole shape consumes the largest working, the rhomb is second and the the twins saw-cut the least.

It has been shown that thermal conduction has an important influence for deformation heat field of metals. Here we make the specimen of twins saw-cut shape as an example. If the tensile time is reduced to 1/2, 1/4 and 1/8 of the original time calculated, at this time, the plastic zone is seen to extend to a position which agrees with the zone in Fig.10. The results of finite element analysis are shown in Figs.12(a), (b) and (c), respectively. It is obvious that the form of isothermal line resembles the form of the plastic zone. The temperature rise of the notch tip is higher and higher, but the influence of thermal conduction on the notch tip is still higher that at other zones since yield previously concentrated in a small area takes place at the notch tip. For the adiabatic situation and with thermal conductivity $K = 0$, the temperature distribution is given in Fig.12(d). It may be seen that the form of isothermal line naturally agrees with the serious zone of deformation and higher temperature rise takes place on the notch tip which follows plastic deformation.

V. CONCLUSIONS

In this paper the temperature distribution all over the metal thin sheet in the process of elastic-plastic deformation was evaluated by the finite element analysis. With an assumption of almost lack of variance in thermal conductivity during less deformation, the results of the heat field calculated from the finite element analysis using Kelvin's equation of thermal conductivity is in better agreement with that surveyed by an infrared themographic.

The ability to calculate the temperature distribution of the metal thin sheet during quasti-static or elastic-plastic deformation is of great importance on the mechanical analysis of metal. This calculation seems to be available for the thermal effect caused by elastic-plastic deformation.

ACKNOWLEDGMENTS

One of the authors (Y.H.) would like to thank Professor Abdus Salam, the International Atomic Energy Agency and UNESCO for hospitality at the International Centre for Theoretical Physics, Trieste.

REFERENCES

1) J.G. Williams, Appl. Mater. Res. 4, 104 (1965) No.2.

2) R. Weichert and K. Schoenert, J. Mech. Phys. Sol. 22, 129 (1974).

3) Y.C. Fung, Foundation of Solid Mechanics (Prentice-Hill Inc., London, 1965) p.388.

4) R.W. Dunlap, E.E. Hucke and D.V. Ragone, Exp. Mech. 8, 154 (1968) No.4.

5) Y. Huang, S.X. Li and C.H. Shih, "Advances in fracture research", Procs. of the 6th Intern. Conf. on Fracture, New Delhi, 4-10 December 1984, p.2.

6) F.R.N. Nabarro, Theory of Crystal Dislocation (Oxford University Press, USA, 1967) p.692.

7) A.O. Tay and P.L.B. Oxley, "Finite element methods in engineering", Proc. 1976 Intern. Conf. on Finite Element Methods in Engineering, Australia (1976) pp.42.1-42.2.

8) P.V. Marcal and I.P. King, Int. J. Mech. Sci. 9, 143 (1967) No.3.

9) D.H. Li, Finite Element Analysis (Scientific Publ. House of China, 1979) p.191.

FIGURE CAPTIONS

Fig.1 The temperature variation of the stainless steel sheet during tensile test.

Fig.2 The experimental value of thermal conductivity for the stainless steel.

Fig.3 Thermal conduction in plate zone R.

Fig.4 Three geometric shapes of hole on specimens, mm .

Fig.5 True stress-strain plot for stainless steel.

Fig.6 Load-time curves for three hole shapes.

Fig.7 Heat field results of finite element analysis, plastic zone extended to boundary, (a), (b) and (c) representing three specimens with various hole shapes.

Fig.8 Photograph of infrared image, plastic zone extended to boundary, (a) and (c) the inverted and (b)-normal.

Fig.9 Isotherms of thermographic, plastic zone extended to boundary, (a), (b) and (c) representing three various hole shapes.

Fig.10 Finite element analysis results of plastic zone during extending, (a), (b) and (c) representing three various hole shapes.

Fig.11 Finite element analysis results of equivalent strain, plastic zone extended to boundary, (a), (b) and (c) representing three various hole shapes.

Fig.12 Finite element analysis results under condition of various rates of tensile and adiabatic process.

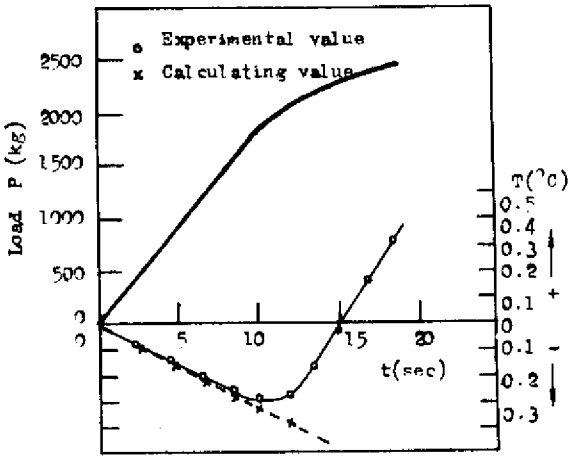

Fig.1

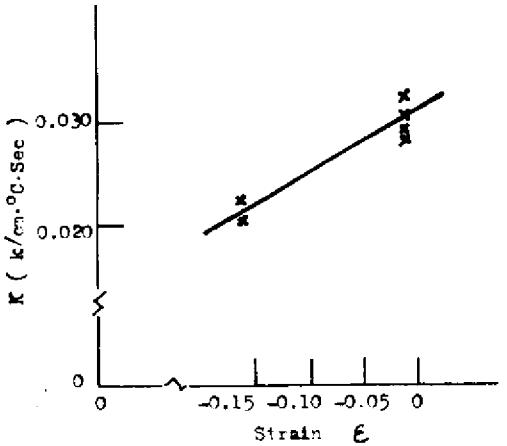

Fig.2

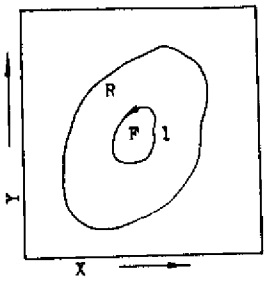

Fig.3

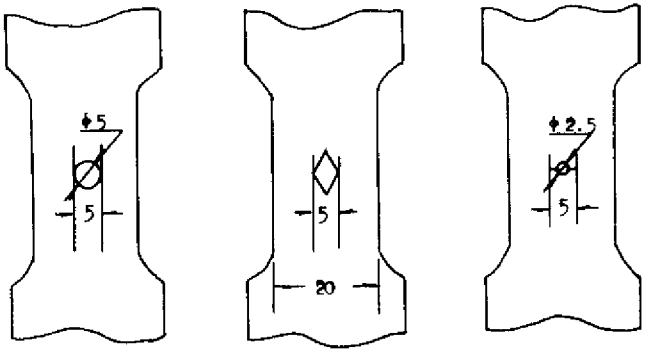

Fig.4

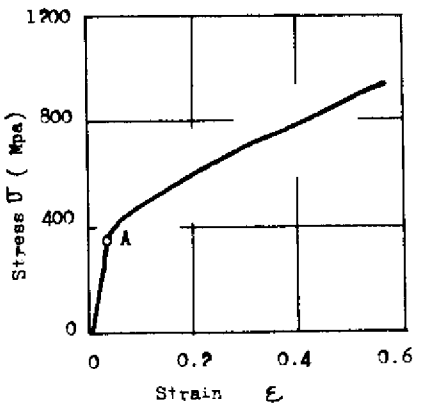

Fig.5

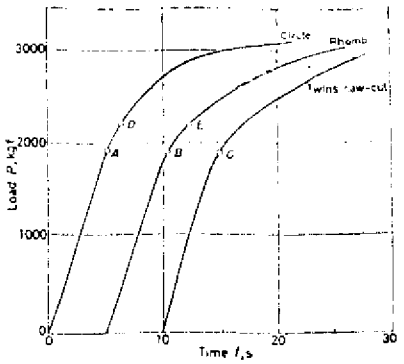

Fig.6

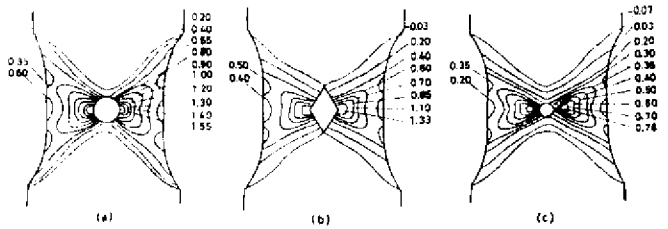

Fig.7

Fig.8

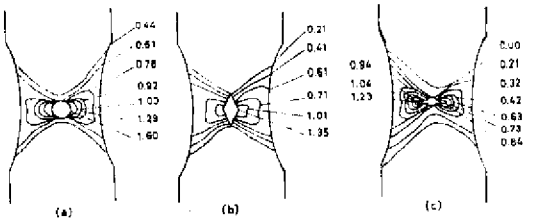

Fig.9

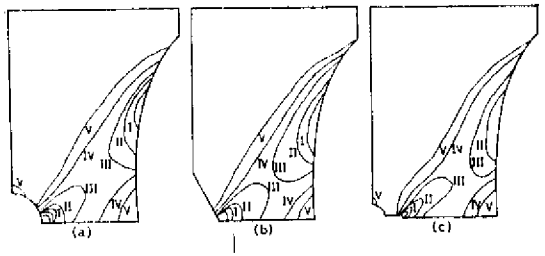

Fig.10

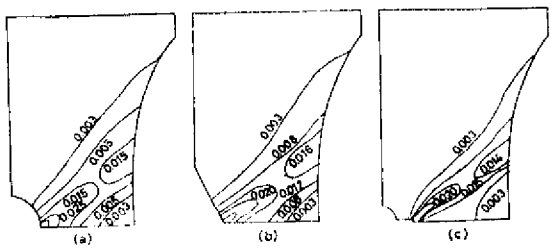

Fig.11

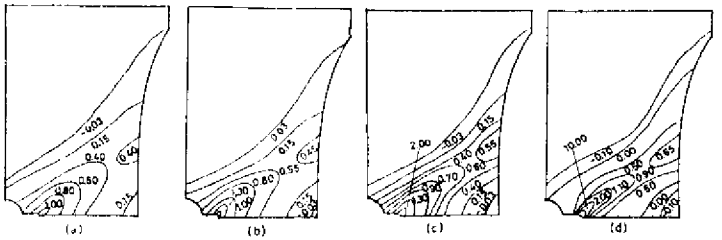

Fig.12